

# First Person Action-Object Detection with EgoNet

Gedas Bertasius<sup>1</sup>, Hyun Soo Park<sup>1</sup>, Stella X. Yu<sup>2</sup>, and Jianbo Shi<sup>1</sup>

<sup>1</sup>University of Pennsylvania, <sup>2</sup>UC Berkeley / ICSI

**Abstract.** Objects afford visual sensation and motor actions. A first person camera, placed at the person’s head, captures unscripted moments of our visual sensorimotor object interactions. Can a single first person image tell us about our momentary visual attention and motor action with objects, without a gaze tracking device or tactile sensors? To study the holistic correlation of visual attention with motor action, we introduce the concept of *action-objects*—objects associated with seeing and touching actions, which exhibit characteristic 3D spatial distance and orientation with respect to the person. A predictive action-object model is designed to re-organize the space of interactions in terms of visual and tactile sensations, which is realized by our proposed EgoNet network. EgoNet is composed of two convolutional neural networks: 1) Semantic Gaze Pathway that learns 2D appearance cues with first person coordinate embedding, and 2) 3D Spatial Pathway that focuses on 3D depth and height measurements relative to the person with brightness reflectance attached. Retaining two distinct pathways enables effective learning from a limited number of examples, diversified prediction from complementary visual signals, and flexible architecture that is functional with RGB image without depth information. We show that our model correctly predicts action-objects in a first person image where we outperform the existing approaches across different datasets.

## 1 Introduction

Our visual sensation is developed along with the neuromotor system while interacting with surrounding objects [1–5]. This tight interplay between visual sensation and motor signal makes spatial scene and object understanding possible through interactions. These interactions between a person and objects are often encoded in a form of the gaze movement and the 3D formation of the objects around that person. For instance, consider a woman entering a canned food corner at a grocery store as shown in Figure 1. When she schemes through hundreds of canned foods to find the tuna can that she looks for, she remains 3-5m from the foods for efficient search. Once she finds the tuna, she approaches it (1-3m), and then reaches her left hand to pick the tuna can (<1m). While she gazes at the expiration date in the label of the can, the distance gets smaller (<0.5m). Not only does the tuna can stimulate her visual attention but it also affects her physical actions, such as head or hand movements.

We define such object as an *action-object*—an object that triggers person’s visual and motor signals. The key properties of the action-object are: (1) it is associated with specific actions such as seeing or touching; (2) it possesses characteristic distance and orientation with respect to the person (i.e 3D formation); and (3) it stimulates person’s visual attention, i.e. the object stays in the particular field of the person’s view. These

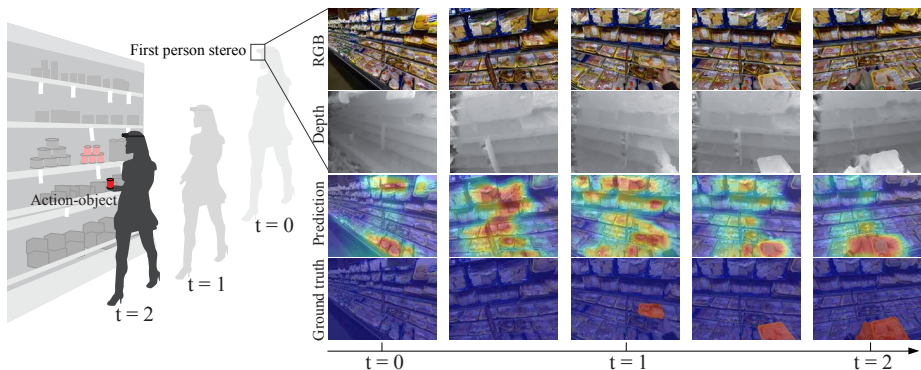


Fig. 1: We predict action-object from the first person RGBD images (best viewed in color) where action-objects are defined as objects that facilitate people’s tactile (grabbing a food package) or visual interactions (watching a TV). Left: a woman approaches a shelf to pick up a food item (red). Right: The food (action-object) is detected progressively as she approaches and reaches her hand to pick it up.

properties provide a strong cue to predict the person’s behavior and also to better understand his visual sensorimotor coordination [1] that plays a critical role in detecting the developmental disabilities such as autism spectrum disorder [6, 7].

A fundamental research question is whether we can build a model that can detect action-objects as we observe a person interacting with his environment without a gaze tracking devices or tactile sensors. This question is challenging despite of recent success of computer vision systems because (a) a person’s gaze direction does not necessarily correspond to action-objects. In other words, not all objects within the person’s field of view are consciously attended. (b) Additionally, there exist infinite spatial configurations of general objects with respect to the person, which makes the task even more challenging. (c) Finally, action-objects are not specific to object category because many object categories can correspond to the same action, e.g., TV and a mirror both afford a seeing action, and therefore, an object specific model may not be able to represent the action-objects. In this paper, we address these challenges by leveraging a first person camera that inherently organizes the space and objects around the person to facilitate his interactions with the environment [8].

The use of a first person camera, placed directly at the source of person-object interaction, is a significant departure from the traditional passive observation from a third person camera such as a surveillance setting. Not only does the first person camera captures what the person sees in terms of object/scene appearance, but it also tells us if she is positioned and oriented herself for a specific action (e.g. seeing or touching). Her relative head orientation indicates what she is attending to, whereas her body position relative to the objects constrains physical feasibility of an action.

Learning to recognize action-objects in the first person view has significant benefits. Action-objects are spatially *normalized* to the first person camera, e.g., regardless of object types, the distance and orientation from objects remains approximately fixed (0.3-0.5m) for a touching action due to the arm length, and therefore there is less vari-

ation in object appearance in the first person images. Our goal is to leverage these first person properties along with the 3D spatial cues to build a model that predicts action-objects. Building such model is different from a classic object detection task because action-object is associated with the actions without explicit object categories. It also differs from a visual saliency detection task because the visual saliency does not necessarily correspond to a specific action. Finally, our action-object task differs from activity recognition tasks because we reason about the actions as a function of objects.

We employ wearable stereo cameras to collect the data containing 2D visual and 3D spatial information around the person, which involves with many object interactions such as cooking, shopping, and dish-washing. The camera wearer who knows action-objects provides the per-pixel binary labels of the first person images. We leverage this data to learn first person 2D and 3D cues of action-objects. We present a novel *EgoNet*, a predictive network model that takes a first person RGB(D) image as an input and learns object’s visual appearance, first person’s gaze, and 3D spatial cues to predict a per-pixel action-object likelihood map. Our network is composed of two distinct pathways: one of which learns visual appearance, and first person gaze cues, and the other pathway that learns 3D spatial relationship of action-objects. We quantitatively demonstrate that these two pathways produce complementary action-object predictions, which exhibits strong predictive and generalization power across datasets.

Our core contributions include (1) the concept of an action-object that links people’s visual attention and motor actions, (2) a first person action-object dataset with the per-pixel annotations provided by the the camera wearer, (3) EgoNet network design that predicts action-objects, which can be effectively applied to various interaction data including children behavior analysis [9].

## 2 Related Work

**First Person Vision.** A first person camera captures what the person sees during her interaction with an object, which has a direct access to her visual attention and motor actions [10]. This first person property has been exploited in various tasks such as summarizing daily activities using a first person video [11, 12], creating a hyper-lapse video [13], detecting objects [14, 15], and recognizing activities [16–20]. In particular, egocentric spatial representations [16, 21] have demonstrated stronger predictive power than that of a third person for activity recognition [16, 17], gaze movement [19, 22] and future ego-motion [23]. Such representations were used for various personalized [6, 24, 25], and social [26, 27] interactions. Unlike prior approaches that used hand-crafted representations for their tasks [19], we directly learn to predict action-objects by integrating object appearances, first person’s gaze, and 3D spatial cues into our design.

**Complementary Object and Activity Recognition in Third Person.** Actions are performed in the context of objects. This coupling provides a complementary cue to recognize actions [28–30]. Some approaches also used low level bag-of-feature models to learn the spatial relationship between objects and activities from a single third person image [31]. Conversely, the activity can provide a functional cue to recognize ob-

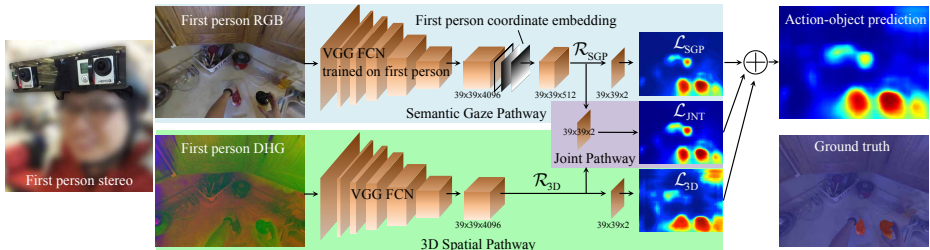


Fig. 2: Our proposed *EgoNet* architecture (best viewed in color) takes as input first person RGB and DHG images, which encode 2D visual appearance and 3D spatial cues, respectively. We design two pathways: the *Semantic Gaze Pathway* that learns visual appearance with first person coordinate embedding and the *3D Spatial Pathway* that learns 3D spatial relationship with respect to the first person. The information from both pathways is combined via the *Joint Pathway* and further integrated by element-wise averaging to predict a per-pixel action-object likelihood.

jects [32–34]. Such a model becomes even more powerful when incorporating the cues of how the object is physically manipulated [35–37]. In addition, object affordance can be learned by simulating human motion in the 3D space [38, 39]. Whereas most of these methods require detected objects or body pose as an input, our work does not need to detect objects or human pose a priori by taking advantage of a first person camera.

**First Person Deep Learning.** Convolutional neural networks have shown remarkable performance achievement on vision tasks including boundary detection, image classification, and semantic segmentation [40–44]. However, due to different visual statistics between natural images and first person images and a limited number of annotated first-person data, first person vision has not been fully exploited by deep learning techniques, except with the pre-trained models as generic feature extractors [20, 23, 45]. Unlike prior work, we propose *EgoNet*, a novel network design using fully convolutional networks [46] that learns first person view, visual appearance and 3D spatial cues, for our newly defined action-object detection task.

### 3 First Person Action-Object RGBD Dataset

We use two stereo GoPro Hero 3 cameras with 100mm baseline to capture first person RGBD videos as shown in Figure 2. The stereo cameras are synchronized manually and each camera is set to 1280×960 with 100 fps. The fisheye lens distortion is pre-calibrated and depth image is computed by estimating disparities between cameras via dense image matching with dynamic programming.

Two subjects participated in capturing their daily interactions with objects in activities such as cooking, shopping, working at their office, dining, buying groceries, dish-washing, and staying in a hotel room. 7 scenes were recorded and 4229 frames with per-pixel action-objects were annotated by the subjects with GrabCut [47]. They also annotated object classes including non-action-objects (a total of 41 object classes). Please find the Supplementary material for the detailed dataset description.

We acknowledge that our dataset has a limited number of sequences, scenes, and subjects. A key question is “can we design a machine that predicts action-objects in general first person scenes using the limited training data?”. We show that our EgoNet has strong generalization power: using our dataset, we learn the common patterns behind people’s object interactions captured in the first person image, and therefore, it can predict in a novel scene. We demonstrate this generalization and predictive power of EgoNet in Section 5.

## 4 EgoNet

In this section, we design *EgoNet*, a predictive network model that detects action-objects from a first person RGB(D) image. This model learns visual and spatial characteristics of the action-objects from our first person action-object RGBD dataset (Section 3).

### 4.1 Motivation

What people see/look at reflects how they are going to act. Conversely, how people act affects what they see at that moment. An action-object measures the momentary visual attention and motor action with objects. This property of the action-object contrasts with most current visual attention studies which focus solely on visual gaze (fixation). We note that the act of looking (gaze) can be random, and does not always lead to seeing (conscious awareness). While gaze is directly measurable from a first person camera, visual attention with intent-to-interact requires directed human annotations. Our major innovation is proposing a learning model for action-object prediction in a first person video using a small set of training examples ( $\approx 4K$ ).

We propose a learning method that holistically integrates a set of visual appearance, head direction, and 3D spatial cues. In contrast, most of the current approaches employ hand-crafted features to predict gaze direction using head/hand pose and motion cues [11, 22, 48]. None of these methods considers the fact that the gaze of a person focuses on the objects in the scene rather than any non-semantic regions in the image [49].

This integration is implemented with two distinct pathways: 1) a *Semantic Gaze Pathway* that learns object visual appearance with first person coordinate embedding; and 2) a *3D Spatial Pathway* that isolates 3D depth and height measurements relative to the person with brightness reflectance attached. Retaining two distinct pathways is beneficial over a network design that trivially concatenates 2D (RGB) and 3D (depth and height) inputs to predict action-objects. First, there are far limited number of depth images for learning action-objects. Bootstrapping *Semantic Gaze Pathway* from the existing RGB object recognition enables more effective learning from a limited number of examples. Second, 2D visual appearance and 3D spatial cues are not entirely orthogonal, as RGB images could predict depth indirectly. The separate pathways allow us to predict action-objects using redundant information from different perspectives analogous to a random forest classifier. Finally, we note that most of the existing datasets do not have 3D information associated with them. Our architecture design is flexible to

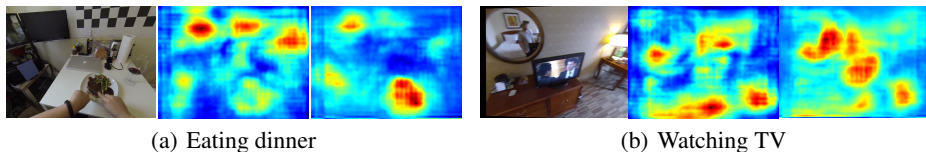


Fig. 3: First person gaze coordinate embedding is beneficial to predict action-objects. The first column depicts an input image, and the second and third column shows activation of fully convolutional networks averaged over 4096 and 512 channels without and with the first person gaze coordinate embedding, respectively. The first person gaze coordinate embedding allows us to accurately localize the regions of the action-objects (the food plate, and the TV).

predict action-object solely via the *Semantic Gaze Pathway* from a first person RGB image without depth information. We verify and characterize our conjecture quantitatively in Section 4.3.

## 4.2 EgoNet Architecture

EgoNet is composed of two pathways: *Semantic Gaze Pathway*, which uses high-level object appearance cues and first person gaze coordinate embedding; and *3D Spatial Pathway* which uses 3D spatial cues to learn prototypical distance and orientation of action-objects. These two pathways are then integrated via the *Joint Pathway*. Finally, the outputs from all three pathways are combined by averaging the response maps of the three pathways, resulting in the per-pixel action-object prediction. The schematics of the EgoNet design is illustrated in Figure 2.

**Semantic Gaze Pathway.** An action-object that stimulates person’s visual attention exhibits two key properties. First, objects with a particular visual appearance attract person’s gaze. For instance, we are more likely to look at the objects that are colored brightly and stand out from the background. Second, the object is often mapped to the specific locations in a first person image due to the 3D geometric configuration of an action-object with respect to the person. For instance, a laptop keyboard is often seen at the bottom of a first person image because we often look down at it while typing with our hands.

We design the *Semantic Gaze Pathway* using a fully convolutional network [46]. It leverages two sources of visual information: object visual semantics and person’s gaze distribution. Our primary conjecture is that different objects are mapped to different locations in the first person image. This conjecture differs from prior work that assumed that a gaze distribution is universal to all object classes (e.g. a center prior) [11, 19]. Object visual semantics are encoded in the  $FC7_{SGP}$  layer of the *Semantic Gaze Pathway* represented by 4096 convolutional output channels. We embed object visual semantics into the first person coordinate system by concatenating the first person gaze coordinate channels with these 4096 channels. This embedding enables us to model the object specific gaze distribution. Note that this gaze distribution is integrated with visual semantics learned by pre-training the network to recognize specific object categories

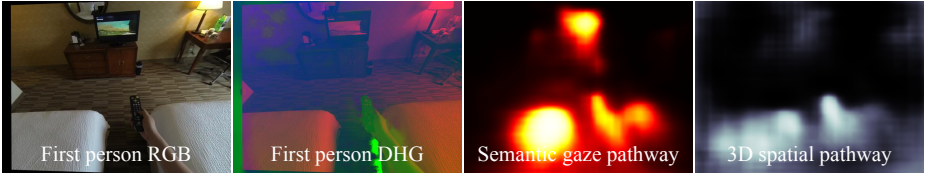


Fig. 4: The figure depicts the outputs of the *Semantic Gaze* and *3D Spatial* pathways with their respective RGB and DHG inputs. Note that the *Semantic Gaze Pathway* “fires” on the semantically meaningful action-objects (a TV), while the *3D Spatial Pathway* focuses on the objects based on their 3D position relative to the person (a remote control).

from the first person images. The visual semantics with the coordinate embedding produces 512 channel output,  $\mathcal{R}_{SGP}(\mathcal{I}^{RGB}) \in \mathbb{R}^{39 \times 39 \times 512}$  where  $\mathcal{I}^{RGB}$  is an RGB first person image. We then attach an extra convolutional layer, which produces per-pixel action-object likelihood,  $\mathcal{L}_{SGP}(\mathcal{I}^{RGB}) \in \mathbb{R}^{39 \times 39 \times 2}$ . The *Semantic Gaze Pathway* is optimized by minimizing softmax loss.

**3D Spatial Pathway.** An action-object also possesses the following 3D spatial properties. It exhibits characteristic distance to the person due to anthropometric constraints, e.g., arm length. For example, when a woman picks up a tuna can, her distance from the can is approximately 0.5m (average arm length of US women is 0.61m). The action-object also has a specific orientation relative to a person because of its design. For instance, when the person carries a cup, she holds it via the handle, which determines the pose of the cup with respect to that person. We hypothesize that these 3D spatial properties can be used to predict the action-objects.

We design the *3D Spatial Pathway* using the VGG fully convolutional network, which learns 3D spatial relationship between a person and action-object. We use depth and height [50] to represent the 3D environment around the person to handle the pitch movements of the head, i.e., the height information tells us about the orientation of the person’s head with respect to 3D environment. In addition, the gray scale image is used to capture the visual appearance cues. Note that we do not use full RGB channels to limit the contribution of 2D visual appearance cues. This diversifies the cues used in the two pathways, which produces complementary predictions.

The learned 3D spatial cues by this pathway are then encoded in the 4096 channel outputs of the  $FC7_{3D}$  layer in the *3D Spatial Pathway*,  $\mathcal{R}_{3D}(\mathcal{I}^{DHG}) \in \mathbb{R}^{39 \times 39 \times 4096}$  where  $\mathcal{I}^{DHG}$  is a 3-channel image composed of depth, height, and gray scale image. An extra convolutional layer is then attached to these 4096 channels to produce per-pixel action-object likelihood,  $\mathcal{L}_{3D}(\mathcal{I}^{DHG}) \in \mathbb{R}^{39 \times 39 \times 2}$ . The *3D Spatial Pathway* is optimized to minimize the softmax loss function.

**Combination of Pathways.** As shown in Figure 4, the two pathways produce different response maps: action-objects based on (1) first person coordinate aware visual appearance, and (2) 3D spatial cues. We combine these two sources of information by integrating the high-level representations from both pathways, which are captured by

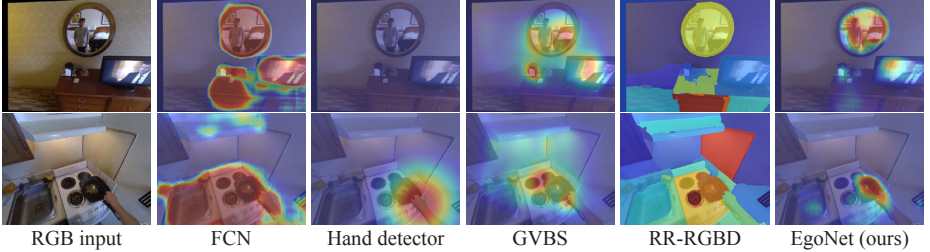


Fig. 5: We qualitatively compare our EgoNet model with other representations (the mirror and the fry pan are the action-objects). The visual saliency methods (GBVS and RR-RGBD) fail because they do not incorporate object level cues. Hand detector fails to identify visual interactions (the mirror) whereas a classic object detector incorrectly treats every object as an action-object. In comparison, the EgoNet accurately predicts action-objects in both cases.

the earlier 512 and 4096 channel outputs ( $\mathcal{R}_{SGP}(\mathcal{I}^{RGB})$  and  $\mathcal{R}_{3D}(\mathcal{I}^{DHG})$ ) from the *Semantic Gaze* and *3D Spatial* pathways, respectively. Additional convolutional layer is used to integrate these outputs (referred to as *Joint Pathway*), which produces the per-pixel action-object likelihood,  $\mathcal{L}_{JNT} \in \mathbb{R}^{39 \times 39 \times 2}$ .

We predict action-objects by averaging the outputs of three pathways ( $\mathcal{L}_{SGP}$ ,  $\mathcal{L}_{3D}$ ,  $\mathcal{L}_{JNT}$ ), which produces a joint response map  $\mathcal{L} \in \mathbb{R}^{39 \times 39 \times 2}$ . This map is upsampled to the original image dimension via a bilinear interpolation. The entire network is jointly optimized by minimizing the per-pixel softmax loss function with respect to the binary ground truth action-object labels.

The predictions by the three pathways are complementary, i.e., one can correct the mistakes made by the other pathway. For instance, in Figure 2, each pathway correctly predicts the action-objects (the steak and the bottle) but also has some false positive predictions. By combining all three pathways, the false positive predictions are assigned to have lower probabilities.

### 4.3 Analysis of EgoNet Architecture

We quantitatively characterize the design factors of our EgoNet architecture in Table 1 using our first person action-object RGBD dataset (Section 3). The black checkmarks indicate the components that were used in the EgoNet, and the red checkmarks indicate which likelihood outputs ( $\mathcal{L}_{SGP}$ ,  $\mathcal{L}_{3D}$ ,  $\mathcal{L}_{JNT}$ ) were used for the final action-object prediction. All the results are evaluated using the standard Max F-Score (MF) and Average Precision (AP) metrics.

**Are Separate Pathways Necessary?** We compare our proposed architecture with a design of trivial concatenation of inputs, RGB, DHG, and first person coordinate embedding. The column 3 indicates that such design produces inferior performance, i.e., 14.4% and 12.6% lower MF and AP compared to ours.



	1	2	3	4	5	6	7	8	9	10
Concatenating RGB, DHG, XY?			✓							
First person object pre-training?	✓		✓				✓	✓	✓	✓
Height?			✓			✓		✓	✓	✓
First person coordinates?			✓		✓		✓	✓	✓	✓
Semantic Gaze Pathway?	✓	✓	✓		✓		✓	✓	✓	✓
3D Spatial Pathway?				✓		✓		✓	✓	✓
Joint Pathway?								✓		✓
Mean max F-score (MF)	0.222	0.244	0.249	0.277	0.299	0.323	0.363	0.372	0.388	<b>0.393</b>
Mean average precision (AP)	0.129	0.162	0.166	0.174	0.206	0.181	0.250	0.253	0.283	<b>0.292</b>

Table 1: We characterize design factors in EgoNet (best viewed in color). Each column represents a particular architecture and each checkmark indicates which components were used for that experiment. The checkmarks that are colored in red indicate which likelihood outputs ( $\mathcal{L}_{SGP}$ ,  $\mathcal{L}_{3D}$ ,  $\mathcal{L}_{JNT}$ ), were used for the final action-object prediction. More than one colored checkmark means that the outputs from several pathways have been combined via the elementwise averaging.

**Is First Person Object Pretraining Necessary?** Objects in the first person view may be seen differently than objects in the natural images [51]. We compare the performance of action-object prediction by *Semantic Gaze Pathway* with and without the first person object pre-training. The columns 5 and 7 demonstrate that the first person object pre-training improves the accuracy by 6.4% (MF) and 4.4% (AP).

**Are First Person Coordinate Embedding Necessary?** In our EgoNet architecture, we embed the first person gaze coordinates to encode the location prior of an action-object. The columns 1 and 7 show that this first person coordinate embedding improves the accuracy (14.1% of MF and 12.1% of AP improvement). In Figure 3, we visualize the activations inside the convolutional layers averaged across the 4096 channels of the *Semantic Gaze Pathway* without (left) and with (right) the first person coordinate embedding. We observe that in the former case, the activations in the network are not consistent with the action-objects (the food plate, and the TV) whereas in the latter case, the activations highlight the action-objects.

**Are 3D Spatial Cues Contributing?** Earlier we claimed that the 3D spatial cues play an important role in action-object prediction task. The columns 7 and 9 in Table 1 shows that incorporating *3D Spatial Pathway* boosts the accuracy by 2.5% (MF) and 3.3% (AP). The height information in our DHG representation also contributes to the performance as it yields 4.6% (MF) and 0.7% (AP) improvement over the design without the height (see column 4 and 6). In Figure 4, we also present qualitative comparisons of what is predicted by the *Semantic Gaze Pathway* and *3D Spatial Pathway*. The *Semantic Gaze Pathway* predicts action-objects based on their visual appearance and person’s gaze distribution (e.g. a TV), whereas the *3D Spatial Pathway* predicts action-objects based on 3D spatial layout around the person (e.g a remote control). This implies that the two pathways provide diverse cues about action-objects, and their combination improves overall action-object detection accuracy.

	cooking		hotel		grocery		desk work		dining		shopping		dishwash		mean	
	MF	AP	MF	AP	MF	AP	MF	AP	MF	AP	MF	AP	MF	AP	MF	AP
FCN [52]	0.091	0.033	0.158	0.054	0.052	0.020	0.225	0.105	0.181	0.084	0.110	0.044	0.077	0.021	0.128	0.052
Hand Det.	0.210	0.085	0.148	0.045	0.161	0.044	0.315	0.142	0.234	0.086	0.106	0.024	0.078	0.012	0.179	0.062
GBVS [53]	0.213	0.113	0.231	0.138	0.043	0.014	0.504	<b>0.502</b>	0.200	0.106	0.116	0.057	0.161	0.088	0.210	0.146
SP	0.366	0.264	0.195	0.084	0.180	0.086	0.394	0.222	0.421	0.327	0.137	0.074	0.267	0.178	0.280	0.176
MCG [54]	0.224	0.113	0.274	0.136	<b>0.243</b>	0.126	<b>0.597</b>	0.389	0.400	0.283	0.200	0.093	0.281	0.170	0.317	0.187
RR-RGBD	0.306	0.182	<b>0.358</b>	<b>0.237</b>	0.188	0.107	0.503	0.377	<b>0.556</b>	<b>0.451</b>	<b>0.404</b>	<b>0.279</b>	0.258	0.180	0.367	0.259
EgoNet	<b>0.474</b>	<b>0.362</b>	0.318	0.206	0.234	<b>0.159</b>	0.523	0.499	0.504	0.423	0.308	0.166	<b>0.386</b>	<b>0.228</b>	<b>0.393</b>	<b>0.292</b>

Table 2: We evaluate predictive power of EgoNet using our first person RGBD dataset. We measure max F-score (MF) and average precision (AP). All the methods (except GBVS, which is unsupervised) were trained on our dataset using the leave-one-out cross validation. The result indicates that EgoNet has the strongest predictive power with at least 2.6% (MF) and 3.3% (AP) gain.

**Is Combination of Pathways Necessary?** The *Joint Pathway* without response averaging performs worse than the combined outputs from the *Semantic Gaze* and *3D Spatial* pathways. Column 8, 9, and 10 show the effects of the *Joint Pathway* and averaging of all pathways. Column 10 is the full model, 8 is without averaging, and 9 is without *Joint Pathway*. Fusing the three pathways by averaging, yields 2.1%, and 3.9% improvement comparing to the designs using a single pathway, which suggests that all three pathways contribute diverse action-object information, which improves the final prediction.

#### 4.4 Implementation Details

We implement EgoNet using Caffe [55]. The *Semantic Gaze* and *3D Spatial* pathways are built upon the VGG fully convolutional network [46]. The *Semantic Gaze Pathway* is pre-trained to predict 41 object classes from our first person action-object dataset while the *3D Spatial Pathway* uses the VGG pre-trained model to diversify the learning capability. We trained our network for 3000 iterations, at the learning rate of  $10^{-6}$ , momentum of 0.9, weight decay of 0.0005, batch size of 20, and the dropout rate of 0.5. To optimize the network, we employed a per-pixel softmax loss with respect to the ground truth action-object annotations. We handle the unbalanced class labels using a gradient weighting scheme [56].

We sequentially train the EgoNet via four steps for the efficient GPU memory footprint in practice. This sequential training allows us to bootstrap a good initialization and regularization which are essential for such large networks. (1) We pre-train the *Semantic Gaze Pathway* for the first person object recognition that enables the network to detect objects from first person RGB images. (2) Next, we independently train *Semantic Gaze Pathway* and *3D Spatial Pathway* to predict action-objects. (3) We then optimize the layers in the *Joint Pathway* while freezing the parameters in the earlier layers. (4) Finally, we jointly optimize the full network except for the parameters in the first 14 convolutional layers of the *Semantic Gaze Pathway* and *3D Spatial Pathway*.

## 5 Results

We evaluate our method both quantitatively and qualitatively across different first person datasets. The main focus of the quantitative evaluation is two-fold: (1) predictive

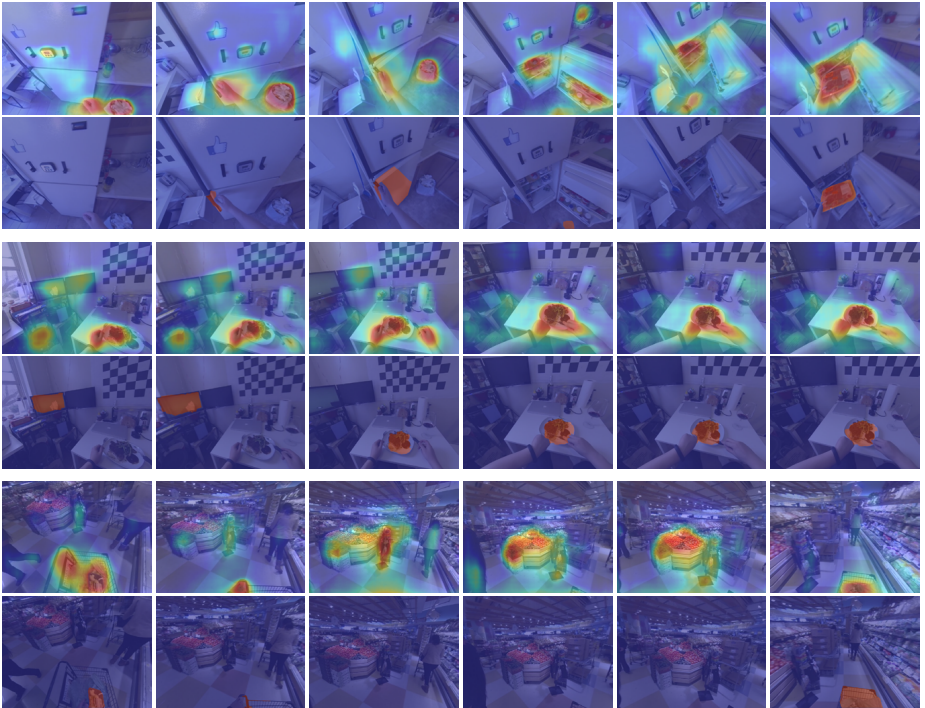


Fig. 6: We illustrate short sequences of our results from our first person RGBD dataset (best viewed in color). The  $1^{st}$ ,  $3^{rd}$ ,  $5^{th}$  rows depict the EgoNet predictions whereas the  $2^{st}$ ,  $4^{th}$ ,  $6^{th}$  rows illustrate ground truth action-objects overlaid on RGB images. Our method predicts what the person will do next even though we have not explicitly trained it to do so. For instance, in column 4 of the  $1^{st}$  row, the EgoNet predicts multiple objects that can be taken out of the fridge. In column 6, the person takes one of these objects. We also note, that even in the cases of false positive prediction (see  $5^{th}$  row), EgoNet makes pretty sensible predictions.

power on our dataset, and (2) generalization power on other datasets. We also qualitatively evaluate our method’s performance on first person YouTube videos that contain various actions, objects, and for some of which, the camera wearer is a non-human, e.g., dog, and on children’s social interaction data.

## 5.1 Quantitative Evaluation of Predictive Power

We evaluate the predictive power of EgoNet using the maximum F-score (MF) and average precision (AP). We compare our approach to the state-of-the-art baseline methods on our first person action-object RGBD dataset. We include the following baseline methods in our comparisons: (1) GBVS [53]: a bottom-up visual saliency prediction method; (2) MCG [54]: a multiscale object segmentation proposal method; (3) Hand detector: a Gaussian distribution around a detected hand trained on our dataset; (4) Spatial Prior (SP): the average action-object location mask obtained from our dataset; (5)

	breakfast		pizza		snack		salad		pasta		sandwich		burger		mean	
	MF	AP	MF	AP	MF	AP	MF	AP	MF	AP	MF	AP	MF	AP	MF	AP
RR-RGB	0.214	0.129	0.194	0.116	0.188	0.113	0.182	0.087	0.179	0.099	0.110	0.044	0.186	0.107	0.189	0.109
MCG [54]	0.387	<b>0.289</b>	0.312	0.204	0.352	0.259	0.321	0.226	0.306	0.208	0.325	0.231	0.312	0.231	0.331	0.235
GBVS [53]	0.294	0.179	0.363	0.259	0.356	0.274	0.426	0.328	0.378	<b>0.282</b>	0.262	0.168	0.343	0.250	0.346	0.249
EgoNet	<b>0.417</b>	0.253	<b>0.408</b>	<b>0.262</b>	<b>0.417</b>	<b>0.287</b>	<b>0.458</b>	<b>0.333</b>	<b>0.395</b>	0.275	<b>0.346</b>	<b>0.252</b>	<b>0.415</b>	<b>0.322</b>	<b>0.408</b>	<b>0.288</b>

Table 3: Quantitative results on GTEA Gaze+ dataset for the fixation prediction task. The dataset contains first person RGB videos of several people cooking 7 different meals. We rely solely on the *Semantic Gaze Pathway* to make our predictions. We show that EgoNet outperforms all the other methods on this dataset by at least 6.2% MF and 3.9% AP. We note that none of these methods were retrained on GTEA Gaze+ dataset in order to test their generalization ability.

FCN [52]: a fully convolutional object detection network trained on our dataset with 41 object classes; and (6) RR-RGBD: a region-based regression method with hand-crafted features. RR-RGBD predicts action-objects using a random forest regressor on the segments provided by the MCG [54] method. The features include region properties such as shape, size, its location in the first person frame, histograms of depth, etc. Many of these features were successfully used in [11, 49, 54]. Please find the Supplementary material for more details of RR-RGBD.

All methods are trained on our dataset except for GBVS which is an unsupervised method. The training is conducted using the leave-one-out cross validation scheme as is standard for first person videos. Based on the results in Table 2, we observe that EgoNet outperforms all baseline methods by at least 2.6% (MF) and 3.3% (AP). FCN performs poorly because it ignores the first person view cues. Hand detector based method fails to identify visual interactions. The results of SP method, indicate that the first person spatial prior is not enough to precisely predict action-objects. Finally, we show that EgoNet also outperforms popular GBVS and MCG methods.

Figure 5 illustrates our qualitative action-object predictions. The visual saliency methods (GBVS and RR-RGBD) do not predict action-objects correctly because they do not use any object-level information. For instance, the RR-RGBD method predicts a rectangular region of wall in the column 4 at the bottom as an action-object. Given that the region is rectangular, RR-RGBD method incorrectly assumes that it’s likely to be an object such as TV. In comparison, the EgoNet was explicitly trained to recognize objects in the pre-training stage, and thus it correctly identifies action-objects. We also observe that while Hand Detector with a Gaussian on top, may detect objects facilitating tactile sensation, it fails with visual sensation (looking at the mirror) whereas our method correctly detects action-objects in both cases. An FCN trained for a classical object detection performs poorly since it treats every object as an action-object without the first person cues. In contrast, our method holistically integrates a set of visual appearance, head direction, and 3D spatial cues, which allows it to detect action-objects with high accuracy.

## 5.2 Quantitative Evaluation on Generalization Power

We quantitatively evaluate the generalization power of EgoNet on GTEA Gaze+ dataset [19]. The GTEA Gaze+ dataset consists of multiple people cooking 7 different meals, with

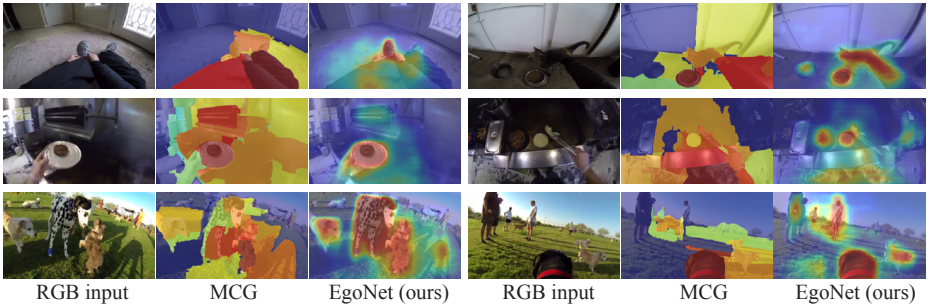


Fig. 7: Our results on 3 first person RGB YouTube videos (best viewed in color). First row depicts a video of a person dressing up and feeding his cat. The second video shows a restaurant chef cooking a meal. The last video is captured by a dog-mounted camera in the park. We show that EgoNet produces better qualitative results than the MCG [53]. We note that both methods were trained on our first person action-object dataset.

their gaze annotations recorded using a wearable eye-tracker. We run our method on 7 videos corresponding to each meal cooking activity. Since GTEA Gaze+ dataset contains only RGB information, our prediction relies solely on *Semantic Gaze Pathway*. The task for this dataset is to predict people’s fixation from the first person frames. To adapt the annotations to an action-object detection task, we threshold a Gaussian with the standard deviation of 60 in pixel at a fixation point and use the resulting mask as a binary ground truth map. We use MF and AP metrics to evaluate the results.

All methods are trained on our first person action-object dataset, and tested on GTEA Gaze+ dataset. The strong generalization ability of EgoNet is critical because the number of existing annotated first person datasets are limited.

In Table 3, our method shows the strongest generalization power compared to RR-RGB, MCG, and GBVS methods. While RR-RGB method exhibits a strong predictive power on our first person RGBD action-object dataset, it achieves poor results on this dataset. Additionally, since the annotations on this dataset capture people’s fixations, our results indicate that the *Semantic Gaze Pathway* implicitly learns to model person’s fixation even if no 3D information is available.

### 5.3 Qualitative Evaluation

We qualitatively demonstrate our method’s results for the videos that capture people’s daily activities and social interactions.

**YouTube Videos.** We use the *Semantic Gaze Pathway* to predict action-object in the first person RGB YouTube videos. These videos include a person dressing up and feeding a cat, a restaurant chef making a dish, and playing in the park from a dog’s first person view. In Figure 7, we compare EgoNet with MCG trained on our first person action-object dataset where EgoNet predicts more semantically meaningful action-objects than MCG. Additionally, we note that due to our method’s ability to generalize, EgoNet can successfully predict action-objects in novel scenes and even from non-human’s view.



Fig. 8: We predict action-objects from the data that captures children’s social interactions. The EgoNet shows strong predictive and generalization power, which detects semantically meaningful action-objects (person, block, and painting) although such scenes are not presented in the training data.

Our model finds action-objects which are important for the first person while classic object detectors would detect all objects indiscriminately.

**Children’s Social Interaction Videos.** Our model has scientific impact on computational behavioral analysis. In particular, it can analyze children’s visual sensorimotor behavior where the early detection of behavioral diseases such as autism spectrum disorder is critical for remedy and rehabilitation. Figure 8 shows action-object prediction on first person children’s interactions [57], which includes playing a card game, building block towers, and playing hide-and-seek. Due to strong generalization power, EgoNet enables qualitatively meaningful predictions even though it has not been trained in this environment.

## 6 Summary

We present a novel concept of an *action-object* to study the holistic relation of visual attention with motor actions using a first person RGB(D) image. We design EgoNet, a predictive network model that detects action-objects by integrating the *Semantic Gaze Pathway* and *3D Spatial Pathway*, both of which leverage 2D and 3D complementary visual cues encoded in the first person image. We demonstrate that our method quantitatively outperforms other methods on our first person action-object RGBD dataset.

We also demonstrate that our model generalizes very well across a variety of diverse datasets. It is readily applicable to many exciting applications such as personalized video dialog creation, video summarization, dexterous hand skill acquisition, and empirical understanding of visual sensorimotor systems of humans and even non-humans.

## References

1. Johansson, R.S., Westling, G., Bäckström, A., Flanagan, J.R.: Eye hand coordination in object manipulation. *Journal of Neuroscience* (2001) [1](#), [2](#)
2. Perone, S., Madole, K.L., Ross-Sheehy, S., Carey, M., Oakes, L.M.: The relation between infants' activity with objects and attention to object appearance. *Developmental Psychology* (2008) [1](#)
3. Vidoni, E.D., McCarley, J.S., Edwards, J.D., Boyd, L.A.: Manual and oculomotor performance develop contemporaneously but independently during continuous tracking. *Experimental Brain Research* (2009) [1](#)
4. Bowman, M.C., Johansson, R.S., Flanagan, J.R.: Eye hand coordination in a sequential target contact task. *Experimental Brain Research* (2009) [1](#)
5. Lazzari, S., Mottet, D., Vercher, J.L.: Eye hand coordination in rhythmical pointing. *Journal of Motor Behavior* (2009) [1](#)
6. Rehg, J.M., Abowd, G.D., Rozga, A., Romero, M., Clements, M.A., Sclaroff, S., Essa, I., Ousley, O.Y., Li, Y., Kim, C., Rao, H., Kim, J.C., Presti, L.L., Zhang, J., Lantsman, D., Bidwell, J., Ye, Z.: Decoding children's social behavior. In: *CVPR*. (2013) [2](#), [3](#)
7. Takarae, Y., Luna, B., Minshew, N.J., Sweeney, J.A.: Visual motion processing and visual sensorimotor control in autism. *Journal of International Neuropsychology Society* (2014) [2](#)
8. Hall, E.T.: A system for the notation of proxemic behaviour. *American Anthropologist* (1963) [2](#)
9. Park, H.S., Jain, E., Sheikh, Y.: 3d gaze concurrences from head-mounted cameras. In: *NIPS*. (2012) [3](#)
10. Kanade, T., Hebert, M.: First person vision. In: *IEEE*. (2012) [3](#)
11. Lee, Y.J., Grauman, K.: Predicting important objects for egocentric video summarization. *IJCV* (2015) [3](#), [5](#), [6](#), [12](#)
12. Lu, Z., Grauman, K.: Story-driven summarization for egocentric video. In: *CVPR*. (2013) [3](#)
13. Kopf, J., Cohen, M.F., Szeliski, R.: First-person hyper-lapse videos. *TOG (SIGGRAPH)* (2014) [3](#)
14. Ren, X., Gu, C.: Figure-ground segmentation improves handled object recognition in egocentric video. In: *CVPR*. (2010) [3](#)
15. Bolaños, M., Radeva, P.: Ego-object discovery. *arxiv:1504.01639* (2015) [3](#)
16. Pirsivash, H., Ramanan, D.: Detecting activities of daily living in first-person camera views. In: *CVPR*. (2012) [3](#)
17. Fathi, A., Farhadi, A., Rehg, J.M.: Understanding egocentric activities. In: *ICCV* [3](#)
18. Taralova, E.H.S., De la Torre, F., Hebert, M.: Temporal segmentation and activity classification from first-person sensing. In: *CVPR Workshop* [3](#)
19. Li, Y., Ye, Z., Rehg, J.M.: Delving into egocentric actions. In: *CVPR* [3](#), [6](#), [12](#)
20. Ryoo, M.S., Rothrock, B., Matthies, L.: Pooled motion features for first person videos. In: *CVPR*. (2015) [3](#), [4](#)
21. Li, C., Kitani, K.M.: Pixel-level hand detection for ego-centric videos. In: *CVPR*. (2013) [3](#)
22. Li, Y., Fathi, A., Rehg, J.M.: Learning to predict gaze in egocentric video. In: *ICCV* [3](#), [5](#)
23. Park, H.S., Hwang, J.J., Niu, Y., Shi, J.: Egocentric future localization. In: *CVPR*. (2016) [3](#), [4](#)
24. Ye, Z., Li, Y., Liu, Y., Bridges, C., Rozga, A., Rehg, J.M.: Detecting bids for eye contact using a wearable camera. In: *FG*. (2015) [3](#)
25. Pusiol, G., Soriano, L., Fei-Fei, L., Frank, M.C.: Discovering the signatures of joint attention in child-caregiver interaction. In: *CogSci*. (2014) [3](#)

26. Fathi, A., Hodgins, J.K., Rehg, J.M.: Social interaction: A first person perspective. In: CVPR. (2012) [3](#)
27. Park, H.S., Jain, E., Sheikh, Y.: 3d social saliency. In: NIPS. (2012) [3](#)
28. Wu, J., Osuntogun, A., Choudhury, T., Philipose, M., Rehg, J.M.: A scalable approach to activity recognition based on object use. In: ICCV. (2007) [3](#)
29. Yao, B., Fei-Fei, L.: Grouplet: A structured image representation for recognizing human and object interactions. In: CVPR. (2010) [3](#)
30. Yao, B., Fei-Fei, L.: Modeling mutual context of object and human pose in human object interaction activities. In: CVPR. (2010) [3](#)
31. Delaitre, V., Sivic, J., Laptev, I.: Learning person-object interactions for action recognition in still images. In: NIPS. (2011) [3](#)
32. Turek, M.W., Hoogs, A., Collins, R.: Unsupervised learning of functional categories in video scenes. In: ECCV. (2010) [4](#)
33. Gall, J., Fossati, A., Van Gool, L.: Functional categorization of objects using real-time markerless motion. In: CVPR. (2011) [4](#)
34. Kjellstrom, H., Romero, J., Kragic, D.: Visual object action recognition: Inferring object affordances from human demonstration. CVIU (2011) [4](#)
35. Gupta, A., Davis, L.S.: Objects in action: An approach for combining action understanding and object perception. In: CVPR. (2007) [4](#)
36. Gupta, A., Satkin, S., Efros, A.A., Hebert, M.: From 3d scene geometry to human workspace. In: CVPR. (2011) [4](#)
37. Rabinovich, A., Vedaldi, A., Galleguillos, C., Wiewiora, E., Belongie, S.: Objects in context. In: ICCV. (2007) [4](#)
38. Fouhey, D.F., Delaitre, V., Gupta, A., Efros, A.A., Laptev, I., Sivic, J.: People watching: Human actions as a cue for single-view geometry. In: ECCV. (2012) [4](#)
39. Yu, L.F., Duncan, N., Yeung, S.K.: Fill and transfer: A simple physics-based approach for containability reasoning. In: ICCV. (2015) [4](#)
40. Bertasius, G., Shi, J., Torresani, L.: High-for-low and low-for-high: Efficient boundary detection from deep object features and its applications to high-level vision. In: ICCV. (2015) [4](#)
41. Krizhevsky, A., Sutskever, I., Hinton, G.E.: Imagenet classification with deep convolutional neural networks. In: NIPS. (2012) [4](#)
42. Donahue, J., Jia, Y., Vinyals, O., Hoffman, J., Zhang, N., Tzeng, E., Darrell, T.: Decaf: A deep convolutional activation feature for generic visual recognition. arxiv:1310.153 (2013) [4](#)
43. Toshev, A., Szegedy, C.: Deeppose: Human pose estimation via deep neural networks. arxiv:1312.4659 (2013) [4](#)
44. Taigman, Y., Yang, M., Ranzato, M., Wolf, L.: Deepface: Closing the gap to human-level performance in face verification. In: CVPR. (2014) [4](#)
45. Park, H.S., Hwang, J.J., Shi, J.: Force from motion: Decoding physical sensation from a first person video. In: CVPR. (2016) [4](#)
46. Simonyan, K., Zisserman, A.: Very deep convolutional networks for large-scale image recognition. arXiv:1409.1556 (2014) [4](#), [6](#), [10](#)
47. Rother, C., Kolmogorov, V., Blake, A.: "grabcut": Interactive foreground extraction using iterated graph cuts. ToG (SIGGRAPH) (2004) [4](#)
48. Bertasius, G., Park, H.S., Shi, J.: Exploiting egocentric object prior for 3d saliency detection. arXiv:1511.02682 (2015) [5](#)
49. Li, Y., Hou, X., Koch, C., Rehg, J., Yuille, A.: The secrets of salient object segmentation. In: CVPR. (2014) [5](#), [12](#)
50. Gupta, S., Girshick, R., Arbeláez, P., Malik, J.: Learning rich features from RGB-D images for object detection and segmentation. In: ECCV. (2014) [7](#)



51. Russakovsky, O., Deng, J., Su, H., Krause, J., Satheesh, S., Ma, S., Huang, Z., Karpathy, A., Khosla, A., Bernstein, M., Berg, A.C., Fei-Fei, L.: ImageNet Large Scale Visual Recognition Challenge. arXiv:1409.0575 (2014) 9
52. Long, J., Shelhamer, E., Darrell, T.: Fully convolutional networks for semantic segmentation. In: CVPR. (2015) 10, 12
53. Harel, J., Koch, C., Perona, P.: Graph-based visual saliency. In: NIPS. (2007) 10, 11, 12, 13
54. Arbeláez, P., Pont-Tuset, J., Barron, J., Marques, F., Malik, J.: Multiscale combinatorial grouping. In: CVPR. (2014) 10, 11, 12
55. Jia, Y., Shelhamer, E., Donahue, J., Karayev, S., Long, J., Girshick, R., Guadarrama, S., Darrell, T.: Caffe: Convolutional architecture for fast feature embedding. arXiv:1408.5093 (2014) 10
56. Xie, S., Tu, Z.: Holistically-nested edge detection. In: ICCV. (2015) 10
57. Park, H.S., Shi, J.: Social saliency prediction. In: CVPR. (2015) 14